Soft Matter

Defect Dynamics in Active Polar Fluids vs. Active Nematics

Journal:	*Soft Matter*
Manuscript ID	SM-ART-06-2022-000830.R1
Article Type:	Paper
Date Submitted by the Author:	15-Sep-2022
Complete List of Authors:	Vafa, Farzan; Harvard University Center of Mathematical Sciences and Applications,

Soft Matter

ARTICLE TYPE

Cite this: DOI: 00.0000/xxxxxxxxxx

Defect Dynamics in Active Polar Fluids vs. Active Nematics†

Farzan Vafa[a]

Received Date
Accepted Date

DOI: 00.0000/xxxxxxxxxx

Topological defects play a key role in two-dimensional active nematics, and a transient role in two-dimensional active polar fluids. Using a variational method, we study both the transient and long-time behavior of defects in two-dimensional active polar fluids in the limit of strong order and overdamped, compressible flow, and compare the defect dynamics with the corresponding active nematics model studied recently. One result is non-central interactions between defect pairs for active polar fluids, and by extending our analysis to allow orientation dynamics of defects, we find that the orientation of $+1$ defects, unlike that of $\pm 1/2$ defects in active nematics, is not locked to defect positions and relaxes to asters. Moreover, using a scaling argument, we explain the transient feature of active polar defects and show that in the steady state, active polar fluids are either devoid of defects or consist of a single aster. We argue that for contractile (extensile) active nematic systems, $+1$ vortices (asters) should emerge as bound states of a pair of $+1/2$ defects, which has been recently observed. Moreover, unlike the polar case, we show that for active nematics, a linear chain of equally spaced bound states of pairs of $+1/2$ defects can screen the activity term. A common feature in both models is the appearance of $+1$ defects (elementary in polar and composite in nematic) in the steady state.

1 Introduction

In the context of biological systems, topological defects are ubiquitous, where they have been associated with cell extrusion[1,2], changes in cell density[3] and morphogenetic processes[4], among others. Here we will study defects in the context of active systems, which are composed of self-propelled active units that move and exert forces on their surrounding by consuming energy, either internal or external[5,6]. One class of active matter is active nematics, which consists of head-tail symmetric active units that tend to align, locally generating nematic (apolar) order [7,8]. For sufficiently large activity, there is a proliferation of topological defects in the nematic texture[8–12], and understanding of the dynamics of topological defects has been advanced by treating the defects as quasiparticles[9,13–19].

Another class of active matter is active polar fluids, which consists of active polar units that tend to align, locally generating polar order[5,20,21]. The phase diagram of active polar fluids has been extensively studied (for example, [21–27]), and defects have been observed in for example[28–32]. In contrast to active nematics, since active polar fluids have long range order[33,34], defects are not spontaneously generated, and if generated due to boundary effect for example, the defects are expected to be transient[21,35,36]. That being said, aspects of dynamics of defects in active polar fluids have been studied in[25,26,32,35,37–39]. Here we study transient dynamics of defects, and give another perspective why they are transient. Applying the same argument to active nematics uncovers a 1D chain of $+1$ defects which screens the activity.

In this paper, we study both the transient and long-time behavior of defects in two-dimensional active polar fluids in the limit of strong order and overdamped, compressible flow. As in[18,19], we consider an approximation for the global texture motivated from the passive case where the defects are widely separated and quasi-static, and use the variational principle to find defect dynamics within this ansatz. Here we shall follow the general approach of[18]. In contrast to previous work on the active nematics model[9,14,15,18,40], in this model we find that there are no active self-propulsion terms for the lowest charge (± 1) energy excitations. Also in contrast to[18], we obtain interactions between two defects that are neither central nor perpendicular to a central force; they are generically non-central. By extending this ansatz to allow orientation dynamics of defects, we find that the orientation of $+1$ defects, unlike that of $\pm 1/2$ defects in active nematics[18], is not locked to defect positions and relaxes to asters, which we confirm with simulations. Moreover, using a scaling argument, we explain the transient feature of active polar defects and show that in the steady state, active polar fluids are either devoid of defects or consist of a single aster. We argue that for contractile

[a] Center of Mathematical Sciences and Applications, Harvard University, Cambridge, MA 02138, USA. E-mail: fvafa@cmsa.fas.harvard.edu

† Electronic Supplementary Information (ESI) available: [details of any supplementary information available should be included here]. See DOI: 10.1039/cXsm00000x/

(extensile) active nematic systems, $+1$ vortices (asters) should emerge as bound states of a pair of $+1/2$ defects, which has been studied in [16,41–46]. Moreover, unlike the polar case, we show that for active nematics, a linear chain of equally spaced bound states of two $+1/2$ defects can screen the activity term. This hints at the existence of stationary lattice of bound states of pairs of $+1/2$ defects in the long term behavior of active nematics, perhaps similar to [44,47]. A common feature in both models is the appearance of $+1$ defects (elementary in polar and composite in nematic) in the steady state.

The paper is organized as follows. We introduce the model in Sec. 2 and in Sec. 3 we review the class of quasi-stationary multi-defect solutions we use to parameterize the dynamics of textures. In Sec. 4 we review the derivation of defect dynamics equations and present our results for the active induced pair-wise interactions. In Sec. 5 we extend our method to study orientation dynamics of defects, and in Sec. 6 we offer an explanation as to why defects are transient and describe the long-time behavior. Finally, in Sec. 7 we compare this model to the active nematics model introduced recently in [18]. Most of the technical details are relegated to Appendices A-C.

2 The Model

We consider a minimal model of a two-dimensional polar order parameter $\mathbf{p}$ described by the free energy [22,48] $\mathscr{F}(\{\mathbf{p}\})$:

$$\mathscr{F}(\{\mathbf{p}\}) = \frac{1}{2}\int dxdy\left[K\ Tr(\nabla\mathbf{p})^2 + g(1-\mathbf{p}^2)^2\right], \tag{1}$$

where K is the Frank constant in the one-constant approximation and g controls the strength of polar order. We assume to be deep in the ordered state ($g\to\infty$), where the coherence length $\xi=\sqrt{K/2g}$ is the smallest relevant lengthscale and $|\mathbf{p}|\approx 1$ except within polar defect cores of size $a\sim\xi$. Although symmetry allows us to write terms that are odd in $\mathbf{p}$, for simplicity of analysis and in order to later connect with a nematic model, we will assume that this contribution can be ignored, for example by imposing $\mathbf{p}\to-\mathbf{p}$ symmetry.

For the dynamics, we consider simplified Toner-Tu theory [33,49] where relaxation towards the minimum of the free energy while advection by compressible flow $\mathbf{v}$ leads to

$$\partial_t p_i + \mathbf{v}\cdot\nabla p_i + \omega_{ij}p_j = -\frac{D}{4K}\frac{\delta\mathscr{F}}{\delta p_i}, \tag{2}$$

where D is the diffusivity and $\omega_{ij}=(\partial_i v_j-\partial_j v_i)/2$ is the vorticity. We would like to comment here that for simplicity we have ignored any explicit couplings between the density ρ and $\mathbf{p}$, and that in principle, ρ can be determined by the continuity equation through $\mathbf{v}$.

In the overdamped limit, $\mathbf{v}=v_0\mathbf{p}$, where v_0 has the dimensions of a speed and represents the speed of an isolated active particle. Then our equations take the form

$$\partial_t p_i + \frac{v_0}{2}\mathbf{p}\cdot\nabla p_i = -\frac{D}{4K}\frac{\delta\mathscr{F}}{\delta p_i}. \tag{3}$$

In Eq. (2) we have dropped the rate of strain alignment term [20,22] because in $2D$ and in the overdamped limit, its effect on dynamics can be represented by renormalizing the advection term. We rescale length with ℓ, where ℓ is the characteristic separation between topological defects, and time with $\tau=\ell^2/D$. We assume that defects are widely separated, that is $\ell\gg\xi$, and thus define the dimensionless small parameter $\varepsilon=\xi/\ell\ll 1$. We also define the dimensionless activity parameter $\lambda=v_0/8D$.

As in [18], it is convenient to adopt the language of complex analysis. In terms of complex coordinates $z=x+iy$ and $\bar z=x-iy$, the complex partial derivatives $\partial=\partial_z=\frac{1}{2}(\partial_x-i\partial_y)$ and $\bar\partial=\partial_{\bar z}=\frac{1}{2}(\partial_x+i\partial_y)$, and the complex order parameter $p=p_x+ip_y$, the (dimensionless) free energy takes the form

$$\mathscr{F}(\{p\}) = \int dzd\bar z\left[4|\partial p|^2+\varepsilon^{-2}(1-|p|^2)^2\right]. \tag{4}$$

Finally, the equation of motion can be written as

$$\partial_t p = \mathscr{I}(p) = -\frac{\delta\mathscr{F}(\{p\})}{\delta\bar p}+\lambda\mathscr{I}_\lambda(p), \tag{5}$$

where

$$\mathscr{I}_\lambda(p) = -(p\partial+\bar p\bar\partial)p. \tag{6}$$

3 Stationary and quasi-stationary textures deep in the ordered state

For simplicity, we first consider the passive case where $\lambda=0$. Then we are interested in solving

$$\partial_t p = -\frac{\delta\mathscr{F}(\{p\})}{\delta\bar p} = 4\partial\bar\partial p + 2\varepsilon^{-2}(1-|p|^2). \tag{7}$$

Since this model was studied in [18], we will simply review it here. The single defect solution is

$$p=\psi(z,\bar z)=A(|z|)\left(\frac{z}{|z|}\right)^\sigma, \tag{8}$$

with the amplitude $A(|z|)$ describing the defect core [50]: as $r\to 0$, $A(r)\propto r$, and for $r\gg\varepsilon$, $A(r)\simeq 1-\frac{\varepsilon^2}{4r^2}$ (see Appendix A for more details about A).

The multi-defect solution takes the form

$$p_0(z,\bar z|\{z_i\}) = e^{i\psi}\prod_i\Psi_i = e^{i\psi}\prod_i A(|z-z_i|)\left(\frac{z-z_i}{|\bar z-\bar z_i|}\right)^{\sigma_i}, \tag{9}$$

where ψ is the phase of p at infinity. This texture satisfies the boundary condition $p\to e^{i\psi}e^{i\varphi\sum_i\sigma_i}$ as $|z|\to\infty$, where φ is the polar angle. In the special case of a charge neutral system, $\sum_i\sigma_i=0$, and so p is constant on the boundary.

In the limit $\varepsilon\to 0$, the multi-defect texture $p_0(z,\bar z|\{z_i\})$ is the minimizer of $\mathscr{F}(p)$ when defects are pinned (see e.g. [51] and references within). In terms of the defect positions z_i, the free energy $\mathscr{F}_0=\mathscr{F}(p_0)$ takes the well-known form

$$\mathscr{F}_0 \approx 2\pi\sum_{i\neq j}\sigma_i\sigma_j\log\frac{|z_j-z_i|}{L}, \tag{10}$$

which describes a Coulomb interaction between defect charges [52], where L is the system size. Due to the Coulomb interaction, even in the absence of any "activity", the defect cores will move to minimize the free energy $\mathscr{F}_0$. Thus even though p_0 textures minimize

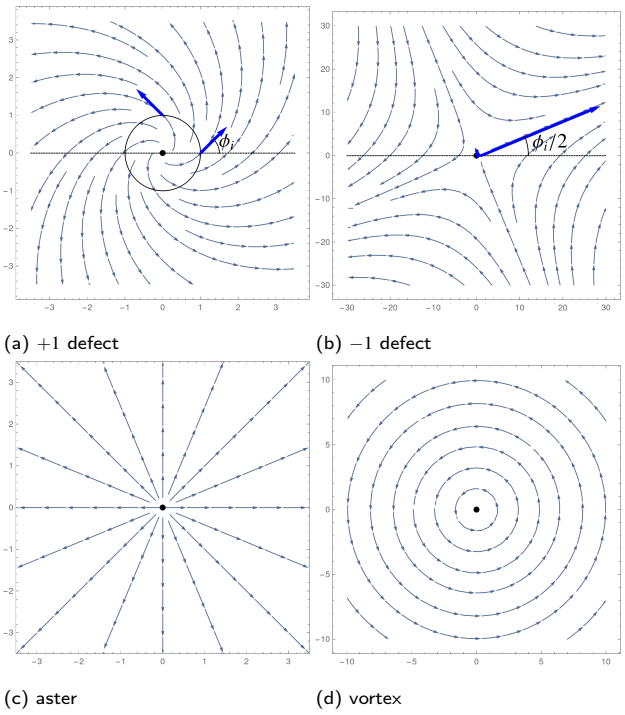

(a) $+1$ defect (b) -1 defect

(c) aster (d) vortex

Fig. 1 Sketches of single defect textures showing the angle ϕ_i (the phase of P_i) for (a) a $+1$ defect where ϕ_i is the angle between P_i and $\hat{r}$, (b) a -1 defect where $\phi_i/2$ is the angle of the separatrix. Special values of ϕ_i are shown in (c) and (d) for a $+1$ defect: (c) is an aster ($\phi_i = 0$), and (d) is a vortex ($\phi_i = \pi/2$).

the free energy when defects are pinned, they are only quasi-static when the defects are no longer pinned.

As noted in [18], near a defect z_i, we can write

$$p_0(z,\bar{z}) \approx P_i \Psi_i(z - z_i, \bar{z} - \bar{z}_i) \,. \tag{11}$$

where

$$P_i = e^{i\phi_i} = e^{i\psi} \prod_{j \neq i} \left(\frac{z_i - z_j}{|z - z_j|} \right)^{\sigma_j} \,. \tag{12}$$

is a phase factor that will play an important role in the active induced dynamics of the defects. See Fig. 1 for a geometrical interpretation.

Finally, we note that for a global rotation, under which $z \to e^{i\eta} z$, the complex order parameter transforms as $p_0 \to p_0 e^{i\eta(1 - \sum_i \sigma_i)}$. This implies that if $\sum_i \sigma_i \neq 1$, we can choose η such that it eliminates the global phase factor ψ. In particular, we cannot eliminate the phase for a single $+1$ defect. This obstruction is not surprising since $+1$ defects are unique among defects in that they are rotationally invariant as $p \propto z$. We will see in our analysis that ψ plays a crucial role for $+1$ defects.

4 Dynamics of active polar defects (interactions)

4.1 Method

We are interested in solving the following PDE:

$$\frac{\partial p}{\partial t} = \mathscr{I}(p) \tag{13}$$

We do so by following the variational method used in [18,19], which we now review. We start by making the ansatz

$$p(z,\bar{z},t) = p_0(z,\bar{z},\{w_a(t)\}) \tag{14}$$

where $w_a(t)$ (perhaps infinitely many) are parameters that need to be specified. (For example, $w_a(t)$ can include the defect positions, but is not strictly limited to them.) Once specified, $w_a(t)$ are computed by minimizing the deviation of dp_0/dt from that described by the equation of motion, Eq. (5). In other words, we minimize the error

$$\begin{aligned} E &= \int d^2 z d\bar{z} \left| \partial_t p(z,\bar{z},t) - \frac{d}{dt} p_0(z,\bar{z}|\{w_a(t)\}) \right|^2 \\ &\approx \int dz d\bar{z} \left| \mathscr{I}(p_0) - \dot{w}_a \frac{\partial p_0}{\partial w_a} \right|^2 \end{aligned} \tag{15}$$

with respect to $\dot{w}_a$, where $\mathscr{I}$ is defined in Eq. (5). Of course, the goodness of our minimization depends on the ansatz and the chosen parameters w_a. We choose our ansatz to be p_0, because we know that when the defects are fixed and when $\lambda = 0$, p_0 is a good solution [51]. Specifically, we assume that the defects are far away from each other and that $\lambda \ll 1$, in which case p_0 is a quasi-static solution to Eq. (5). Taking into account that $\lambda \neq 0$ and the defects are not infinitely far away from each other leads to motion of the defects, and we will assume that the time-dependence of p is only through the defect positions $z_i(t)$, and that the motion is slow. In other words, we will make the ansatz

$$p(z,\bar{z},t) = p_0(z,\bar{z},\{z_i(t)\}) \tag{16}$$

where we have chosen $w_a(t)$ to be $z_i(t)$, the defect positions.

Doing so, one finds that [18]

$$\mathscr{M}_{ij} \dot{z}_j + \mathscr{N}_{ij} \dot{\bar{z}}_j = -\frac{\partial \mathscr{F}_0}{\partial \bar{z}_i} + \lambda \mathscr{U}_i \,, \tag{17}$$

where

$$\mathscr{M}_{ij} = \int d^2 z [\bar{\partial}_i \bar{p}_0 \partial_j p_0 + \bar{\partial}_i p_0 \partial_j \bar{p}_0] \tag{18}$$

$$\mathscr{N}_{ij} = \int d^2 z [\bar{\partial}_i \bar{p}_0 \bar{\partial}_j p_0 + \bar{\partial}_i p_0 \bar{\partial}_j \bar{p}_0] \,. \tag{19}$$

are the mobility matrices,

$$\mathscr{F}_0 = -2\pi \sum_{i \neq j} \sigma_i \sigma_j \ln \frac{|z_i - z_j|}{L} \,, \tag{20}$$

is the Coulomb free energy, and

$$\mathscr{U}_i = \int d^2 z [\bar{\partial}_i \bar{p}_0 \mathscr{I}_\lambda + \bar{\partial}_i p_0 \bar{\mathscr{I}}_\lambda] \,. \tag{21}$$

The mobility matrices $\mathscr{M}_{ij}$ and $\mathscr{N}_{ij}$ have been calculated in [18] to be

$$\mathscr{M}_{ij} \approx \pi \sigma_i \sigma_j \ln \frac{L}{r_{ij}} \tag{22}$$

$$\mathscr{N}_{ij} \approx 0 \,. \tag{23}$$

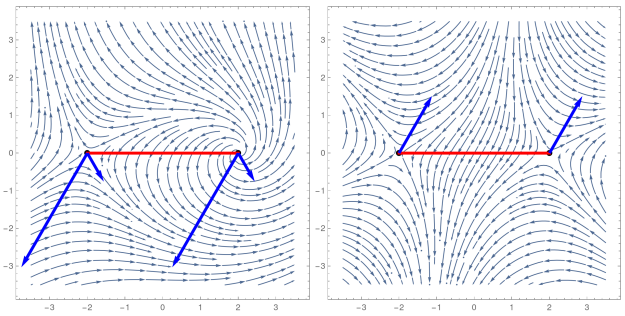

(a) -1 and $+1$ defects (b) -1 and -1 defects

Fig. 2 Sketches of the active forces f_{ij} for $\lambda > 0$. The blue arrows denote the two components of the active force f_{ij}, and the red line joins the center of the two defects. For each pair, $f_{ij} = f_{ji}$, and the net forces are generically non-central.

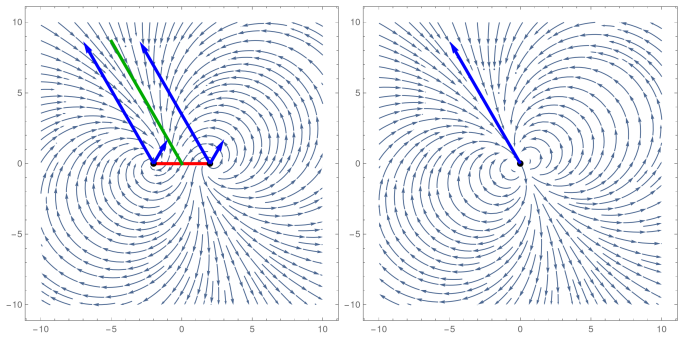

(a) Two $+1$ defects (b) A single $+2$ defect

Fig. 3 Sketches of active forces with $\lambda > 0$ for (a) two $+1$ defects, and (b), for a single $+2$ defect (the "self-propulsion" force). The forces for both cases are essentially in the same direction.

Before proceeding, we would like to emphasize that in order to determine z_i, we are doing a global fit within our ansatz that finds the z_i that minimizes the error. That is to say, although we interpret z_i as the positions of defects, z_i are simply parameters in our ansatz for the global texture that act as a proxy for the defect positions, and similarly $\dot{z}_i$ are not the true velocities of the defects. If we were interested in calculating the exact defect velocities, then we could do so with a local calculation which tracks the zeros of p. However, we are interested in how p evolves everywhere, not just at specific points, which is why we minimize the error E in Eq. (15). Note that the fact that our equations depend on the system size L is not surprising given we are doing a global fit in a region of size L. And, we have the freedom, if we are interested, to focus on the physics in a subregion of size $\ell < L$ by minimizing Eq. (15) in this subregion.

4.2 Interactions

In Appendix B, we show that $\mathscr{U}_i$ (defined in Eq. (21)) can be explicitly written in terms of the defect positions as

$$\lambda \mathscr{U}_i = -8\pi \ln \frac{L}{a} \lambda \bar{P}_i \delta_{\sigma_i,2} + \sum_{j\neq i} f_{ij}, \tag{24}$$

where in terms of the unit vector $\hat{z}_{ij} = (z_i - z_j)/|z_i - z_j|$ and its complex conjugate $\hat{\bar{z}}_{ij}$,

$$f_{ij} = \frac{1}{2}\lambda \sigma_i \sigma_j \hat{z}_{ij} \left(P_i \hat{z}_{ij}^{\sigma_i - 1} I_{ij}^{(1)} - \bar{P}_i \hat{\bar{z}}_{ij}^{\sigma_i - 1} I_{ij}^{(2)} \right) \tag{25}$$

with

$$I_{++}^{(1)} = I_{--}^{(1)} = 2\pi$$

$$I_{+-}^{(1)} = I_{-+}^{(1)} = 2\pi \ln \frac{L}{r_{ij}} + \mathscr{O}(L^0)$$

$$I_{++}^{(2)} = 2\pi \ln \frac{L}{r_{ij}} + \mathscr{O}(L^0); \quad I_{--}^{(2)} = 0$$

$$I_{+-}^{(2)} = I_{-+}^{(2)} = 2\pi \,. \tag{26}$$

The first term in Eq. (24) is the "self-propulsion" of a $+2$ defect along the $\bar{P}_i$ direction, where P_i was defined in Eq. (12). Of course, we should not take this term too seriously, because a $+2$ defect can be interpreted as a bound state of two $+1$ defects, which is unstable because of the Coulomb repulsion. The second term in Eq (24) is the active induced pair-wise interaction, and its leading dependence on distance r_{ij} between two defects i and j is $\ln L/r_{ij}$.

We now examine the net force. Since $I_{ij}^{(1)} \neq I_{ij}^{(2)}$, then f_{ij} is a generic non-central force; in particular, it is also not orthogonal to the line connecting the two defects. We also comment that since $f_{ij} = f_{ji}$, then the defect pair moves together, as if it is a bound object. Another feature is that for a pair of -1 defects, there is no dependence on the distance between the defects, unlike in cases of the neutral pair or pair of $+1$ defects. See Fig. 2 and Fig. 3 for sketches.

We have learned that two $+1$ defects exert the same force on each other (same magnitude and direction), as if they're bound. In the limit that these defects are really close to each other, then there is no reason a priori to expect that they are actually bound, as our assumptions no longer hold. However, interestingly enough, the two defects behave as if they're a $+2$ defect, a bound state of two $+1$ defects, which is "self-propelled" in the same direction, along its separatrix, consistent with the behavior of a $+2$ defect (see Fig. 3). This did not have to be the case, and does not hold for the other defect pairs.

5 Orientation dynamics

In the previous section, we ignored orientation dynamics. We now incorporate orientation dynamics and sketch out the argument here (the details of the computation are in Appendix C). For simplicity, we consider a single defect of charge σ at the origin, in which case our ansatz is

$$p_0 = e^{i\psi(t)} \left(\frac{z}{|z|} \right)^{\sigma}, \tag{27}$$

where now the phase $\psi(t)$ is dynamical. Choosing $w_a(t) = \psi(t)$ in Eq. 15 leads to

$$\int d^2z |\frac{\partial p}{\partial \psi}|^2 \dot{\psi} = \frac{\lambda}{2} \int d^2z \frac{\partial \bar{p}}{\partial \psi} \mathscr{I}_\lambda + c.c \tag{28}$$

and upon evaluation in a region of size ℓ near the defect, where $a \ll \ell \ll L$ and a is the core size,

$$\pi \ell^2 \dot{\psi} = -2\pi\lambda\ell \sin\psi \delta_{\sigma,1} \implies \dot{\psi} = -2\frac{\lambda}{\ell} \sin\psi \delta_{\sigma,1} \,. \tag{29}$$

Only the solution for $+1$ defects is nontrivial, which for completeness is given by

$$\psi(t) = 2\,\mathrm{arccot}\left(e^{\frac{2\lambda}{\ell} t} \cot\left(\frac{\psi(0)}{2} \right) \right) \,. \tag{30}$$

Note that we can interpret Eq. 29 as relaxational dynamics

$$\dot{\psi} = -\frac{2}{\ell} \frac{dV}{d\psi} \tag{31}$$

for the potential $V = -\lambda \cos\psi$ (see Fig. 4 for a plot). Thus for $\lambda > 0$, the defect will relax to an aster ($\psi = 0$), and for $\lambda < 0$, the defect will relax to an inward-pointing aster ($\psi = \pi$).*. In other words, there is a preferred phase. Stable asters have been observed in related simulations[25,26,35,39,53,54], as well as analyzed in related models[37–39,55,56].

We also check our theory with simulations. We evolve an isolated $+1$ defect for nonzero $\lambda = 1$, where initially the phase $\psi(0) = \pi/2$. We computed the phase in two different ways: a local computation, which locates the $+1$ defect and measures the phase, and a global computation, which calculates the defect position and phase by minimizing in a region of size $\ell = 30a \ll L = 300a$ the deviation of our ansatz p_0 from the measured p_0, which is basically equivalent minimizing Eq. (15), as we did in deriving Eq. (29). We find that initially and at long times, the two different measurements of the phase agree, and even though they are not identical in the middle, they both are similar. Moreover, we checked our measured global definition of $\psi(t)$ vs that predicted from theory obtained by integrating Eq. (31), and find remarkable agreement (see Fig. 5).

Given that our method suggests that there appear to be two different stationary solutions for $+1$ defects (aster or inward-pointing aster, depending on the sign of λ), it raises the question whether these solutions are stationary solutions of Eq. (5). By inspection, $+1$ defects, in particular asters or inward-pointing asters, are indeed stationary solutions of Eq. (5).

Since the phase appears to be important, it is natural to ask if we can modify our ansatz in Eq. (16) to take into account the phase, for example by taking $\Psi_i \to e^{i\phi_i f(|z-z_i|)}\Psi_i$, where for example as in[57] $f(|z-z_i|) = e^{i\gamma_i \ln|z-z_i|}$ †. We leave this analysis to future work.

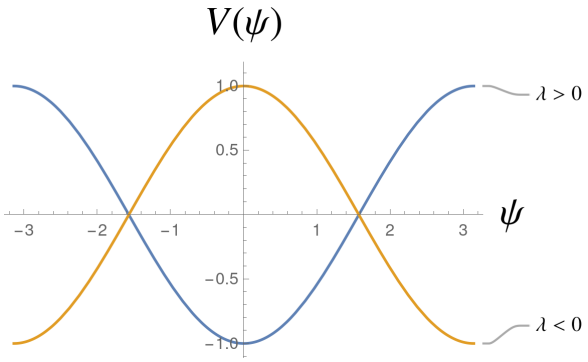

Fig. 4 Plot of $V(\psi)$ for $\lambda > 0$ and $\lambda < 0$. Extrema are at $\psi = 0, \pi$. Minimum for $\lambda > 0$ is at $\psi = 0$, whereas minimum for $\lambda < 0$ is at $\psi = \pi$.

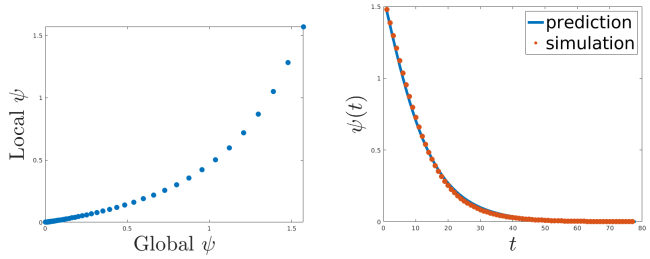

(a) $+1$ defect (b) -1 defect

Fig. 5 Dynamics of the phase $\psi(t)$ of a single $+1$ defect for $\lambda > 0$ with $\psi(0) = \pi/2$. In (a), plot of local computation vs global computation of the phase ψ for a single $+1$. Their ending points are the same, but they are not identical in the middle. In (b), theoretical prediction vs simulation of $\psi(t)$.

6 Stationary solution through scaling argument

In this paper, we have focused on defects. Here we make contact with the discussion contained in[21], and provide another perspective about why defects are transient in active polar fluids.

We make use of a scaling argument. By inspection, there is a scaling symmetry; that is, solutions obey‡

$$p(z,t;\lambda) = p(z/\beta, t/\beta^2; \beta\lambda) \,. \tag{32}$$

We are interested in the stationary, longtime behavior, which means that we are looking for p such that for any t

$$\lim_{\gamma\to\infty} \frac{\partial}{\partial t} p(z, \gamma^2 t; \lambda) = 0 \,. \tag{33}$$

From our scaling relation in Eq. 32, choosing $\beta = \gamma$ is equivalent to finding p such that

$$\lim_{\gamma\to\infty} \frac{\partial}{\partial t} p(z/\gamma, t; \gamma\lambda) = 0 \,. \tag{34}$$

We thus look for steady states for large λ. For large λ, the advection term in Eq. (5) dominates, and thus long-time stationary

* Note that there is a symmetry of our system when $\lambda \to -\lambda$ and $p \to -p$ symmetry.

† We do not assume this form of f as this modified ansatz leads to an infinite free energy addition.

‡ For notational convience, we drop the explicit dependence on g. Explicitly, g scales as $p(z,t;g,\lambda) = p(z/\beta, t/\beta^2; \beta^2 g, \beta\lambda)$. Since we are in the deep nematic limit, $g \to \infty$, so it is unaffected by rescaling. But for finite g, this is how it would scale.

states satisfy

$$\partial_t p = -\lambda(p\partial + \bar{p}\bar{\partial})p = 0\,. \tag{35}$$

We will now show that the only solutions to the above equation other than constant p are a single aster or inward-pointing aster, which as we commented in Sec. 5 satisfies the above equation. Because we are deep in the ordered phase, our ansatz is $p = \frac{f(z)}{\bar{f}(\bar{z})}$. Then

$$\partial_t p = -\lambda(p\partial + \bar{p}\bar{\partial})p = -\frac{\lambda}{\bar{f}^2}(f\partial f - \bar{f}\bar{\partial}\bar{f}) \tag{36}$$

which vanishes only if $\partial(f^2) = c_1$, where $c_1 \in \mathbb{R}$. Therefore, $f^2 = c_1 z + c_2$, and so p is constant if $c_1 = 0$, and otherwise

$$p = e^{i\psi}\frac{(z-z_i)^{1/2}}{(\bar{z}-\bar{z}_i)^{1/2}} \tag{37}$$

where either $\psi = 0$ (aster) or $\psi = \pi$ (inward pointing aster), depending on the sign of λ; no other ψ is allowed. Note that this single aster stationary state is consistent with the single vortex to aster transition, as in Eq. (31). We have thus provided another perspective for transient behavior of defects.

7 Comparison with active nematics model

In this section, we compare our model to the active nematics model studied in [18]. Both models consider the dynamics of topological defects of an order parameter (polar or nematic) deep in the ordered phase and in the overdamped limit. One might be misled to think that since we can use similar techniques to study topological defects in both models, then the behavior would be similar. Here we will show that the type of topological defect (polar vs nematic), *due to activity*, leads to drastic differences in the dynamics. By studying and comparing these models in depth, we can learn which features are common resulting from topological defects and which are specific to polar vs. nematic order. In particular, we will see that for the same choices of defect charges and positions, unlike in the passive case, activity leads to different forces. Moreover, the orientation dynamics are rather different in the active case in the two cases. These differences lead to trivial stationary solutions in the polar case as opposed to the nematic case, which exhibit non-trivial stationary solutions.

7.1 Type of order and activity

In the passive case (absence of activity), the two models are mathematically equivalent, except that the nematic case admits half-integral defects, whereas the polar case admits only integer defects. In the active setting, however, the dependence of the flow field on the order parameter is different. In the overdamped limit, in the case of nematic order, $\mathbf{v} = \alpha\nabla\cdot\mathbf{Q}$, where α is a measure of activity, and in the case of polar order, $\mathbf{v} = \lambda\mathbf{p}$. This difference in dependence of length scaling implies that in the nematic model, α cannot be scaled out of the problem, but in the polar model, λ can be scaled out. To summarize, the main differences between the two models arise from the interplay between the type of order and activity, which we now turn to.

7.2 Forces

Here we compare the active forces. In the active nematics case, a $+1/2$ defect, the smallest allowed energy excitation, is "self-propelled", whereas in the active polar case, a ±1 defect, the smallest allowed energy excitation, is not "self-propelled"; instead, a $+2$ defect is "self-propelled". Another difference between these two models arise in the pair-wise interactions induced by activity. In the active nematics case, the active forces are central for a $(+1/2,+1/2)$ pair, and for the other pairs are orthogonal to line connecting the defects. Also, the forces for $(+1/2,-1/2)$ pair are non-reciprocal. All of these forces fall off as $1/r$, where r is the distance between the defects, and the magnitude depends on the geometry, that is, overall phase of Q. In contrast, in the case of active polar, the active forces are neither central forces nor orthogonal to the line connecting the two defects. For each pair of defects, the active forces are also always equal in magnitude and point in the same direction. Similar to active nematic, the magnitude of the force depends on the orientation of the defect, i.e., the phase of p.

7.3 Orientation dynamics / solutions

In this paper, we learned that $+1$ asters (inward-pointing asters) are stationary solutions and that they are stable for $\lambda > 0$ ($\lambda < 0$). It is natural to ask whether in the nematic model there can be stationary $+1$ defect configurations, and does the existence of solutions, or stability, depend on the phase of the defects. We show that indeed solutions exist, and the type of solution depends on the phase of the defects.

We first check to see what happens if we incorporate orientation dynamics into the active nematics model. In terms of the complex order parameter $Q = Q^{xx} + iQ^{xy}$, the active nematics model has the following equation of motion,

$$\partial_t Q = \mathscr{I}(Q) = -\frac{\delta\mathscr{F}(\{Q\})}{\delta\bar{Q}} + \alpha\mathscr{I}_\alpha(Q)\,, \tag{38}$$

where

$$\frac{\delta\mathscr{F}(\{Q\})}{\delta\bar{Q}} = -4\bar{\partial}\partial Q - 2\varepsilon^{-2}(1-|Q|^2)Q \tag{39}$$

$$\mathscr{I}_\alpha(Q) = -(\partial Q\partial Q + \bar{\partial}\bar{Q}\bar{\partial}Q) + (\partial^2 Q - \bar{\partial}^2\bar{Q})Q \tag{40}$$

We work in the deep nematic limit ($\varepsilon \to 0$). For simplicity, we consider a single defect of charge $\sigma = \pm1/2$ at the origin, in which case our ansatz is

$$Q_0 = e^{i\psi(t)}\left(\frac{z}{\bar{z}}\right)^\sigma\,, \tag{41}$$

where now the phase $\psi(t)$ is dynamical. Minimizing the error

$$E = \int d^2z\,d\bar{z}\left|\partial_t Q(z,\bar{z},t) - \frac{d}{dt}Q_0(z,\bar{z}|\psi(t))\right|^2$$

$$\approx \int dz\,d\bar{z}\left|\mathscr{I}(Q_0) - \dot{\psi}\frac{\partial Q_0}{\partial\psi}\right|^2 \tag{42}$$

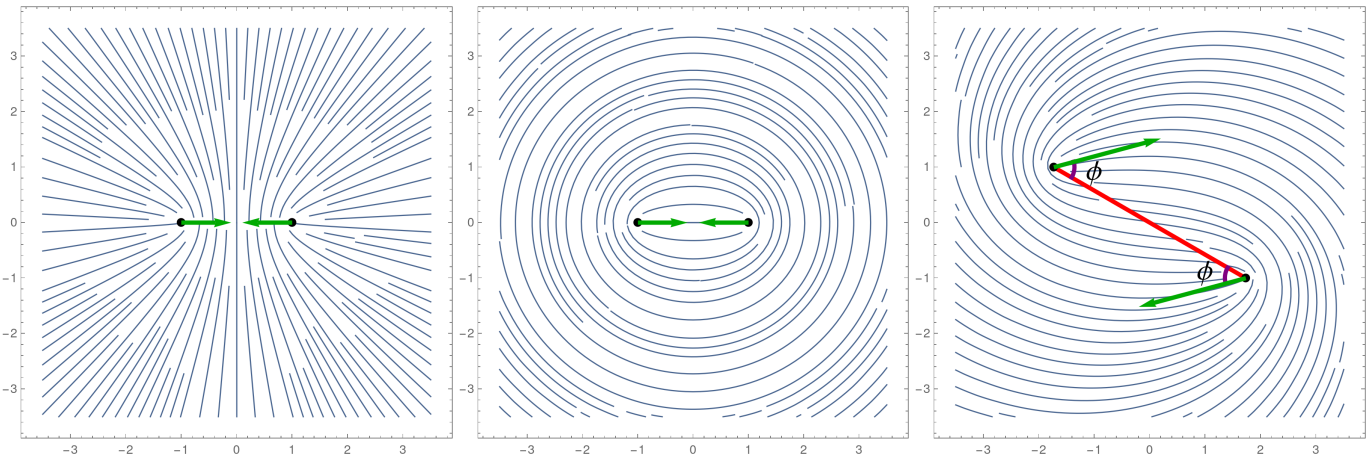

(a) Aster bound state (b) Vortex bound state (c) Spiral bound state

Fig. 6 In active nematics model, sketches of bound state of two $+1/2$ defects. In (a), bound aster state in extensile system when $\psi = 0$, (b), bound vortex state in contractile system when $\psi = \pi$, and in (c), bound spiral state in contractile system when $0 < \psi < \pi/2$.

with respect to $\dot{\psi}$ (the analogue of Eq. (15)) leads to

$$\int d^2z |\frac{\partial Q_0}{\partial \psi}|^2 \dot{\psi} = \frac{\alpha}{2} \int d^2z \frac{\partial \bar{Q}_0}{\partial \psi} \mathscr{I}_\alpha + c.c \tag{43}$$

(the analogue of Eq. (17)). We now evaluate both sides of this equation in a region near the defect of size ℓ. As before,

$$\int d^2z |\frac{\partial Q_0}{\partial \psi}|^2 = \pi \ell^2 \tag{44}$$

We now evaluate the RHS. We have

$$\int d^2z \frac{\partial \bar{Q}_0}{\partial \psi} \mathscr{I}_\alpha + c.c = \tag{45}$$

$$-i \int d^2z [-\sigma^2 (\frac{Q_0}{z^2} - \frac{\bar{Q}_0}{\bar{z}^2}) + \sigma(\sigma-1)(\frac{Q_0}{z^2} - \frac{\bar{Q}_0}{\bar{z}^2})] + c.c$$

$$= 0 \tag{46}$$

which implies that

$$\dot{\psi} = 0 \tag{47}$$

and we thus learn that the phase is frozen, in accordance with the expectation in [18]. Here there is no preferred orientation, unlike in the active polar case, where asters or anti-asters are preferred, depending on the sign of λ.

In related models, $+1$ defect states consisting of two $+1/2$ defects have been observed in active nematics [42,44,45], and in [16,46], it was argued that the type of $+1$ defect was determined by the activity: asters in extensile systems, and vortices in contractile systems. This observation is related to our result of finding a stationary $+1$ defect in the active polar model, as we will now see. We now review and present another argument for the existence and stability of a stationary defect pair of two $+1$ defects in the active nematics case.

Let's consider two $+1/2$ defects situated on the real axis. For simplicity, let's assume that the orientations of the $+1/2$ defects, which anti-align [18,44,45,58], are along the real axis, so they either point away from each other (phase is 0), or toward each other (phase is π). There are four forces: the defect drag force, the repulsive Coulomb force, the self-propulsion, and the active induced pair-wise force. We will ignore the defect drag force and active induced pair-wise force because they renormalize the velocity and Coulomb force, respectively. In this case, for $\alpha > 0$ (contractile), the $+1/2$ defects move with constant velocity in the direction of their phase, and for $\alpha < 0$ (extensile), the $+1/2$ defects move with constant velocity in the opposite direction of their phase. Therefore, at a unique separation r_*, the repulsive Coulomb force can balance the attractive self-propulsion force depending on the sign of α and the phase. The configuration is stationary for either extensile system and phase of 0 or contractile system and phase of π. In the former, the two $+1/2$ defects form a bound aster state, and in the latter, they form a bound vortex state (see Fig. 6). This argument was pointed out in [16,43,46].

Moreover, this bound state is stable to transverse fluctuations of the polarization [16]. Here we present an alternative argument. If the defects are not exactly aligned, one would naively think that the self-propulsion will cause the $+1/2$ defects to go away from each other. However, we will now show that as the defects move, the orientation readjusts in such a way that it leads to inward spiral motion of the pair of defects. From arguments presented in [18], in terms of this phase ϕ (the angle of the orientation, that is, the deviation from radial line connecting the two defects), the solution takes the form

$$Q(z,t) = e^{i\phi} \frac{z - z_i(t)}{|z - z_i(t)|} \frac{z - z_j(t)}{|z - z_j(t)|} \tag{48}$$

where z_i and z_j are the positions of defects i and j, respectively. The orientation $Q_i(t)$ of defect i is simply

$$Q_i(t) = e^{i\phi} \frac{z_i(t) - z_j(t)}{|z_i(t) - z_j(t)|} \tag{49}$$

Since $+1/2$ defects are self-propelled along their orientation, in the direction of Q_i, then they will always move at a constant angle

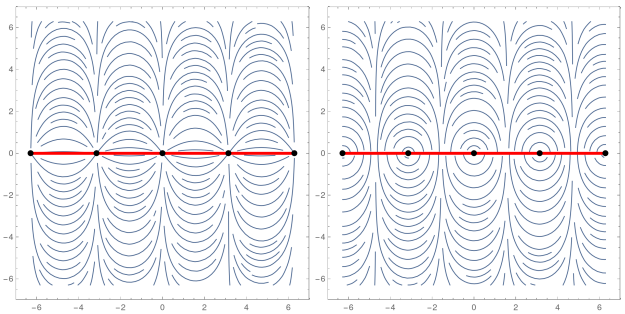

(a) Asters (b) Vortices

Fig. 7 Configuration of 1D chain of equally spaced $+1$ defects for active nematics model that screens the activity term.

ϕ relative to the radial line connecting the two defects. Thus for example in contractile system, if ϕ is sufficiently close to 0, and the activity is not too large, then the two defects will simply spiral towards each other (see Fig. 6). The solution is thus stable, but not stationary.

Given that it seems that a composite made of a pair of $+1/2$ defects is a stationary solution for the active nematic model and far away it looks like an aster or vortex, it is natural to ask if an aster or vortex is actually a solution to Eq. (38). By inspection, indeed a nontrivial solution is $Q = \pm\frac{z}{\bar{z}}$ (as one can easily check that the active term $\mathscr{I}_\alpha = 0$), where the $+$ sign corresponds to an aster and the $-$ sign corresponds to a vortex. Note that this solution of aster or vortex is consistent with the picture in Fig. 6, as any other phase results in a non-stationary state. Thus a single aster or a vortex is indeed a stationary solution to Eq. (38).

Screening of activity term by $+1$ defects in active nematics is similar to what we found in active polar fluids. In active polar fluids, this configuration is the only configuration that screens the active term, thus explaining the transient behavior of defects. Is this the case in active nematics or are there more general configurations that screen the active term? Or can we extend this solution to allow multiple defects? A natural place to look for this (ignoring the passive forces) is to look for configurations that screen the active term ($\mathscr{I}_\alpha = 0$), as in the case of single aster/vortex. In the polar case, a single aster was the only defect configuration that screened the active term. Here we will see that the situation (and solution) is more interesting for a nematic system.

We are thus interested in solving

$$\mathscr{I}_\alpha = 0\,, \tag{50}$$

where

$$\mathscr{I}_\alpha = -\partial Q\partial Q - \bar{\partial}\bar{Q}\bar{\partial}Q + (\partial^2 Q - \bar{\partial}^2\bar{Q})Q\,. \tag{51}$$

Deep in the ordered phase, $Q = \pm e^{i(f(z)+\bar{f}(\bar{z}))}$, and so

$$iQ\left(\partial^2 f e^{2if} + \bar{\partial}^2\bar{f}e^{-2i\bar{f}}\right) = 0 \tag{52}$$

Other than the constant solution, the unique solution is

$$f(z) = -i\ln\sin k(z - z_0) \tag{53}$$

where without loss of generality we can assume $k \in \mathbb{R}$ by rotation of z coordinate if necessary and place the origin at z_0. Therefore,

$$Q = \pm e^{i(f(z)+\bar{f}(\bar{z}))} = \pm\frac{\sin kz}{\sin k\bar{z}}\,. \tag{54}$$

Notice that this vanishes at $z = n\pi/k$, for $n \in \mathbb{Z}$, and near each zero, $Q \sim \pm\frac{z}{\bar{z}}$. We thus have an infinite chain of $+1$ nematic defects on the real axis, separated by π/k. Because of the sign of Q, either the defects are all asters (when the sign is positive), or the defects are all vortices (when the sign is negative). These configurations are depicted in Fig. 7.

Ignoring the Coulomb term, we have analytically found a stationary $1D$ lattice solution. For example, in the geometry of a thin annulus (or equivalently, long channel with periodic boundary conditions), we can imagine that the boundary condition balances the Coulomb forces. In any case, this shows that $\mathscr{I}_\alpha = 0$ has a much more interesting set of solutions than $\mathscr{I}_\lambda = 0$, and deserves further study, pointing to the importance of defects in active nematic systems as opposed to active polar systems.

Conflicts of interest

There are no conflicts to declare.

Acknowledgements

I would like to thank M. Cristina Marchetti for many valuable comments on this manuscript. In addition, I have benefited from discussions with Mark Bowick, Sattvic Ray, and Boris Shraiman.

This work was supported in part by the NSF through grants DMR-1938187 and PHY-0844989.

Appendices

A Single defect solution

Stationary textures in the limit of zero activity ($\lambda = 0$) minimize free energy and hence solve [48,50]

$$\frac{\delta\mathscr{F}}{\delta\bar{p}} = -\nabla^2 p - 2\varepsilon^{-2}(1 - |p|^2)p = 0\,. \tag{55}$$

We look for a solution for a single defect of charge σ of the form

$$p = A(r)e^{i\sigma\varphi}\,. \tag{56}$$

$A(r)$ would thus satisfy

$$A''(r) + \frac{A'}{r} + \left(2\varepsilon^{-2} - \frac{\sigma^2}{r^2} - 2\varepsilon^{-2}A^2\right)A = 0\,. \tag{57}$$

For example, for $\sigma = \pm 1$, $A(r)$ can be approximated as [50]

$$A(r) = \tilde{r}\sqrt{\frac{.68 + .28\tilde{r}^2}{1 + .82\tilde{r}^2 + .28\tilde{r}^4}}\,, \tag{58}$$

where $\tilde{r} = r/\varepsilon$. As $r \to 0$, $A(r) \propto r$, and for $r \gg \varepsilon$, $A(r) \simeq 1 - \frac{\varepsilon^2}{4r^2}$. The defect core size a, which is the length scale over which A goes from 0 to 1, is of the order $a \sim \varepsilon$.

B Computation of $\mathscr{U}_i$

We are interested in computing

$$\mathscr{U}_i = \int d^2z \bar{\partial}_i \bar{p}_0 \mathscr{I}_\lambda + \int d^2z \bar{\partial}_i p_0 \bar{\mathscr{I}}_\lambda = I_1 + I_2 \,, \tag{59}$$

where

$$I_1 = -\int d^2z \bar{\partial}_i \bar{p}_0 p_0 \partial p_0 - \int d^2z \bar{\partial}_i p_0 p_0 \partial \bar{p}_0 \tag{60}$$

$$I_2 = -\int d^2z \bar{\partial}_i p_0 \bar{p}_0 \bar{\partial} \bar{p}_0 - \int d^2z \bar{\partial}_i \bar{p}_0 \bar{p}_0 \bar{\partial} p_0 \,. \tag{61}$$

Substituting for p_0, we find that

$$I_1 = \frac{1}{2}\sum_j \int d^2z p_0 \frac{\sigma_i \sigma_j}{(\bar{z}-\bar{z}_i)(z-z_j)} \tag{62}$$

$$I_2 = -\frac{1}{2}\sum_j \int d^2z \bar{p}_0 \frac{\sigma_i \sigma_j}{(\bar{z}-\bar{z}_i)(\bar{z}-\bar{z}_j)} \tag{63}$$

It is convenient to rewrite the above as

$$I_1 = \frac{1}{2}\int d^2z p_0 \frac{\sigma_i^2}{|z-z_i|^2} + \frac{1}{2}\sum_{j\neq i}\int d^2z p_0 \frac{\sigma_i \sigma_j}{(\bar{z}-\bar{z}_i)(z-z_j)} \tag{64}$$

$$I_2 = -\frac{1}{2}\int d^2z \bar{p}_0 \frac{\sigma_i^2}{(\bar{z}-\bar{z}_i)^2} - \frac{1}{2}\sum_{j\neq i}\int d^2z \bar{p}_0 \frac{\sigma_i \sigma_j}{(\bar{z}-\bar{z}_i)(\bar{z}-\bar{z}_j)} \tag{65}$$

The first term for I_1 vanishes by phase integral. The first term for I_2 is only non-zero for $\sigma_i = 2$, in which case (since we are assuming that defects are well-separated), we can approximate

$$\begin{aligned} -\frac{1}{2}\int d^2z \bar{p}_0 \frac{\sigma_i^2}{(\bar{z}-\bar{z}_i)^2} &\approx -\delta_{\sigma_i,2}\frac{1}{2}\bar{P}_i \int d^2z \frac{(\bar{z}-\bar{z}_i)^2}{|z-z_i|^2}\frac{4}{(\bar{z}-\bar{z}_i)^2} \\ &= -8\pi \bar{P}_i \delta_{\sigma_i,2} \ln \frac{L}{a} \end{aligned} \tag{66}$$

where a is the defect core size and L is the system size. We can identify this term as the self-propulsion of a $+2$ defect. In the following, we will explicitly be assuming that $\sigma_i = \pm 1$, so this term does not appear. Thus we can write

$$I_1 \approx \frac{1}{2}\sum_j P_{ij}\int d^2z \frac{(z-z_i)^{\sigma_i}}{|z-z_i|^{\sigma_i}}\frac{(z-z_j)^{\sigma_j}}{|z-z_j|^{\sigma_j}}\frac{\sigma_i\sigma_j}{(\bar{z}-\bar{z}_i)(z-z_j)} \tag{67}$$

$$I_2 \approx -\frac{1}{2}\sum_j \bar{P}_{ij}\int d^2z \frac{(\bar{z}-\bar{z}_i)^{\sigma_i}}{|z-z_i|^{\sigma_i}}\frac{(\bar{z}-\bar{z}_j)^{\sigma_j}}{|z-z_j|^{\sigma_j}}\frac{\sigma_i\sigma_j}{(\bar{z}-\bar{z}_i)(\bar{z}-\bar{z}_j)} \,, \tag{68}$$

where

$$P_{ij} = \prod_{r\neq i,j}\frac{(z_i-z_r)^{\sigma_r}}{|z_i-z_r|^{\sigma_r}} \,. \tag{69}$$

First shifting $z \to z+z_j$ and then rescaling $z \to z_{ij}z$, we have

$$I_1 = \frac{1}{2}\sum_j \sigma_i\sigma_j P_{ij}\left(\frac{z_{ij}}{|z_{ij}|}\right)^{\sigma_i+\sigma_j} I_{ij}^{(1)} \tag{70}$$

$$I_2 = -\frac{1}{2}\sum_j \sigma_i\sigma_j \bar{P}_{ij}\left(\frac{\bar{z}_{ij}}{|z_{ij}|}\right)^{\sigma_i+\sigma_j-2} I_{ij}^{(2)} \tag{71}$$

where

$$I_{ij}^{(1)} = \int d^2z \frac{(z-1)^{\sigma_i}}{|z-1|^{\sigma_i}}\frac{z^{\sigma_j}}{|z|^{\sigma_j}}\frac{1}{\bar{z}-1}\frac{1}{z} \tag{72}$$

$$I_{ij}^{(2)} = \int d^2z \frac{(\bar{z}-1)^{\sigma_i}}{|z-1|^{\sigma_i}}\frac{\bar{z}^{\sigma_j}}{|z|^{\sigma_j}}\frac{1}{\bar{z}-1}\frac{1}{\bar{z}} \tag{73}$$

are integrals that need to be computed. For notation, let $+(-)$ index denote plus (minus) defect. Using techniques utilized in[18], we find that

$$\begin{aligned} I_{++}^{(1)} &= I_{--}^{(1)} = 2\pi \\ I_{+-}^{(1)} &= I_{-+}^{(1)} = 2\pi \ln\frac{L}{r_{ij}} + \mathscr{O}(L^0) \\ I_{++}^{(2)} &= 2\pi \ln\frac{L}{r_{ij}} + \mathscr{O}(L^0); \quad I_{--}^{(2)} = 0 \\ I_{+-}^{(2)} &= I_{-+}^{(2)} = 2\pi \end{aligned} \tag{74}$$

To summarize, $\mathscr{U}_i$ can be written explicitly in terms of the defect positions as

$$\lambda \mathscr{U}_i = -8\pi \ln\frac{L}{a}\lambda \bar{P}_i \delta_{\sigma_i,2} + \sum_{j\neq i} f_{ij}, \tag{75}$$

where

$$f_{ij} = \frac{1}{2}\sigma_i\sigma_j\left(P_{ij}\hat{z}_{ij}^{\sigma_i+\sigma_j}I_{ij}^{(1)} - \bar{P}_{ij}\hat{\bar{z}}_{ij}^{\sigma_i+\sigma_j-2}I_{ij}^{(2)}\right) \tag{76}$$

can be interpreted as the active induced pair-wise force on defect i due to defect j. f_{ij} can be rewritten as

$$f_{ij} = \frac{1}{2}\sigma_i\sigma_j\hat{z}_{ij}\left(P_{ij}\hat{z}_{ij}^{\sigma_i+\sigma_j-1}I_{ij}^{(1)} - \bar{P}_{ij}\hat{\bar{z}}_{ij}^{\sigma_i+\sigma_j-1}I_{ij}^{(2)}\right) \tag{77}$$

or equivalently as

$$f_{ij} = \frac{1}{2}\sigma_i\sigma_j\hat{z}_{ij}\left(P_i\hat{z}_{ij}^{\sigma_i-1}I_{ij}^{(1)} - \bar{P}_i\hat{\bar{z}}_{ij}^{\sigma_i-1}I_{ij}^{(2)}\right) \tag{78}$$

C Orientation dynamics computations

For simplicity, we consider a single defect of charge σ at the origin, in which case our ansatz is

$$p_0 = e^{i\psi(t)}\left(\frac{z}{|z|}\right)^{\sigma} \,, \tag{79}$$

where now the phase $\psi(t)$ is dynamical. Choosing $w_a(t) = \psi(t)$ in Eq. 15 leads to

$$\int d^2z |\frac{\partial p_0}{\partial \psi}|^2 \dot{\psi} = \frac{\lambda}{2}\int d^2z \frac{\partial \bar{p}_0}{\partial \psi}\mathscr{I}_\lambda(p_0) + c.c, \tag{80}$$

where the Coulomb term vanishes because there is only one defect. We now evaluation both sides of the above equation in a region of size ℓ near the defect, where $a \ll \ell \ll L$ and a is the core size. We first evaluate the LHS. Since $|\frac{\partial p_0}{\partial \psi}| = 1$, then

$$\int d^2z |\frac{\partial p_0}{\partial \psi}|^2 = \pi\ell^2 \,. \tag{81}$$

We now evaluate the RHS. We have

$$\frac{\lambda}{2}\int d^2z\frac{\partial\bar{p}_0}{\partial\psi}\mathscr{I}_\lambda(p_0)+c.c=-\frac{\lambda}{2}\int d^2z\frac{\partial\bar{p}_0}{\partial\psi}(p_0\partial+\bar{p}_0\bar{\partial})p_0+c.c$$

$$=i\frac{\lambda}{2}\frac{\sigma}{2}\int d^2z(\frac{p_0}{z}-\frac{\bar{p}_0}{\bar{z}})+c.c\,. \qquad (82)$$

By phase integral, the above vanishes unless $p_0=e^{i\psi}\frac{z}{|z|}$, that is, $\sigma=1$. Thus

$$\frac{\lambda}{2}\int d^2z\frac{\partial\bar{p}_0}{\partial\psi}\mathscr{I}_\lambda(p_0)+c.c=-\frac{\lambda}{2}\sin\psi\delta_{\sigma,1}\int d^2z\frac{1}{|z|}+c.c$$

$$=-2\pi\lambda\ell\sin\psi\delta_{\sigma,1}\,. \qquad (83)$$

Putting it all together,

$$\pi\ell^2\dot{\psi}=-2\pi\lambda\ell\sin\psi\delta_{\sigma,1}\implies\dot{\psi}=-2\frac{\lambda}{\ell}\sin\psi\delta_{\sigma,1}\,. \qquad (84)$$

Notes and references

1 T. B. Saw, A. Doostmohammadi, V. Nier, L. Kocgozlu, S. Thampi, Y. Toyama, P. Marcq, C. T. Lim, J. M. Yeomans and B. Ladoux, *Nature*, 2017, **544**, 212.

2 K. Kawaguchi, R. Kageyama and M. Sano, *Nature*, 2017, **545**, 327.

3 K. Copenhagen, R. Alert, N. S. Wingreen and J. W. Shaevitz, *Nature Physics*, 2021, **17**, 211–215.

4 Y. Maroudas-Sacks, L. Garion, L. Shani-Zerbib, A. Livshits, E. Braun and K. Keren, *Nature Physics*, 2021, **17**, 251–259.

5 M. C. Marchetti, J.-F. Joanny, S. Ramaswamy, T. B. Liverpool, J. Prost, M. Rao and R. A. Simha, *Reviews of Modern Physics*, 2013, **85**, 1143.

6 R. Aditi Simha and S. Ramaswamy, *Phys. Rev. Lett.*, 2002, **89**, 058101.

7 S. Ramaswamy, R. A. Simha and J. Toner, *EPL (Europhysics Letters)*, 2003, **62**, 196.

8 A. Doostmohammadi, J. Ignés-Mullol, J. M. Yeomans and F. Sagués, *Nature communications*, 2018, **9**, 3246.

9 L. Giomi, M. J. Bowick, X. Ma and M. C. Marchetti, *Physical review letters*, 2013, **110**, 228101.

10 S. P. Thampi, R. Golestanian and J. M. Yeomans, *Physical review letters*, 2013, **111**, 118101.

11 L. Giomi, *Physical Review X*, 2015, **5**, 031003.

12 A. Doostmohammadi, T. N. Shendruk, K. Thijssen and J. M. Yeomans, *Nature communications*, 2017, **8**, 15326.

13 F. C. Keber, E. Loiseau, T. Sanchez, S. J. DeCamp, L. Giomi, M. J. Bowick, M. C. Marchetti, Z. Dogic and A. R. Bausch, *Science*, 2014, **345**, 1135–1139.

14 V. Narayan, S. Ramaswamy and N. Menon, *Science*, 2007, **317**, 105–108.

15 L. M. Pismen, *Physical Review E*, 2013, **88**, 050502.

16 S. Shankar, S. Ramaswamy, M. C. Marchetti and M. J. Bowick, *Physical review letters*, 2018, **121**, 108002.

17 S. Shankar and M. C. Marchetti, *Phys. Rev. X*, 2019, **9**, 041047.

18 F. Vafa, M. J. Bowick, M. C. Marchetti and B. I. Shraiman, *Multi-defect Dynamics in Active Nematics*, 2020.

19 Y.-H. Zhang, M. Deserno and Z.-C. Tu, *Phys. Rev. E*, 2020, **102**, 012607.

20 S. Ramaswamy, *Annu. Rev. Condens. Matter Phys.*, 2010, **1**, 323–345.

21 H. Chaté, *Annual Review of Condensed Matter Physics*, 2020, **11**, 189–212.

22 W. Kung, M. Cristina Marchetti and K. Saunders, *Phys. Rev. E*, 2006, **73**, 031708.

23 L. Giomi, T. B. Liverpool and M. C. Marchetti, *Phys. Rev. E*, 2010, **81**, 051908.

24 L. Giomi and M. C. Marchetti, *Soft Matter*, 2012, **8**, 129–139.

25 A. Gopinath, M. F. Hagan, M. C. Marchetti and A. Baskaran, *Phys. Rev. E*, 2012, **85**, 061903.

26 K. Gowrishankar and M. Rao, *Soft Matter*, 2016, **12**, 2040–2046.

27 L. Chen, C. F. Lee and J. Toner, *Nature communications*, 2016, **7**, 12215.

28 C. Dombrowski, L. Cisneros, S. Chatkaew, R. E. Goldstein and J. O. Kessler, *Phys. Rev. Lett.*, 2004, **93**, 098103.

29 I. H. Riedel, K. Kruse and J. Howard, *Science*, 2005, **309**, 300–303.

30 A. Sokolov, I. S. Aranson, J. O. Kessler and R. E. Goldstein, *Phys. Rev. Lett.*, 2007, **98**, 158102.

31 H. H. Wensink, J. Dunkel, S. Heidenreich, K. Drescher, R. E. Goldstein, H. Löwen and J. M. Yeomans, *Proceedings of the National Academy of Sciences*, 2012, **109**, 14308–14313.

32 V. Schaller and A. R. Bausch, *Proceedings of the National Academy of Sciences*, 2013, **110**, 4488–4493.

33 J. Toner and Y. Tu, *Phys. Rev. Lett.*, 1995, **75**, 4326–4329.

34 J. Toner and Y. Tu, *Phys. Rev. E*, 1998, **58**, 4828–4858.

35 K. Husain and M. Rao, *Phys. Rev. Lett.*, 2017, **118**, 078104.

36 B. Mahault, X.-c. Jiang, E. Bertin, Y.-q. Ma, A. Patelli, X.-q. Shi and H. Chaté, *Phys. Rev. Lett.*, 2018, **120**, 258002.

37 K. Kruse, J. F. Joanny, F. Jülicher, J. Prost and K. Sekimoto, *Phys. Rev. Lett.*, 2004, **92**, 078101.

38 K. Kruse, J. Joanny, F. Jülicher, J. Prost and K. Sekimoto, *The European physical journal. E, Soft matter*, 2005, **16**, 5—16.

39 J. Elgeti, M. E. Cates and D. Marenduzzo, *Soft Matter*, 2011, **7**, 3177–3185.

40 T. Sanchez, D. T. Chen, S. J. DeCamp, M. Heymann and Z. Dogic, *Nature*, 2012, **491**, 431.

41 G. Duclos, C. Erlenkämper, J.-F. Joanny and P. Silberzan, *Nature Physics*, 2017, **13**, 58.

42 N. Kumar, R. Zhang, J. J. de Pablo and M. L. Gardel, *Science advances*, 2018, **4**, eaat7779.

43 T. Turiv, J. Krieger, G. Babakhanova, H. Yu, S. V. Shiyanovskii, Q.-H. Wei, M.-H. Kim and O. D. Lavrentovich, *Science Advances*, 2020, **6**, eaaz6485.

44 K. Thijssen, M. R. Nejad and J. M. Yeomans, *Phys. Rev. Lett.*, 2020, **125**, 218004.

45 D. J. G. Pearce, J. Nambisan, P. W. Ellis, A. Fernandez-Nieves and L. Giomi, *Phys. Rev. Lett.*, 2021, **127**, 197801.

46 K. Thijssen and A. Doostmohammadi, *Phys. Rev. Research*, 2020, **2**, 042008.

47 A. U. Oza and J. Dunkel, *New Journal of Physics*, 2016, **18**, 093006.

48 P. G. De Gennes and J. Prost, *The physics of liquid crystals*, Clarendon Press, Oxford, 1993.

49 J. Toner, Y. Tu and S. Ramaswamy, *Annals of Physics*, 2005, **318**, 170 – 244.

50 L. M. Pismen, *Vortices in nonlinear fields: From liquid crystals to superfluids, from non-equilibrium patterns to cosmic strings*, Oxford University Press, 1999, vol. 100.

51 F. Pacard and T. Rivière, *Linear and Nonlinear Aspects of Vortices: The Ginzburg-Landau Model*, Birkhäuser, Boston, MA, 2000.

52 P. M. Chaikin and T. C. Lubensky, *Principles of condensed matter physics*, Cambridge university press, 2000.

53 I. S. Aranson and L. S. Tsimring, *Phys. Rev. E*, 2005, **71**, 050901.

54 I. S. Aranson and L. S. Tsimring, *Phys. Rev. E*, 2006, **74**, 031915.

55 H. Youn Lee and M. Kardar, *Phys. Rev. E*, 2001, **64**, 056113.

56 S. Sankararaman, G. I. Menon and P. B. Sunil Kumar, *Phys. Rev. E*, 2004, **70**, 031905.

57 X. Tang and J. V. Selinger, *Soft Matter*, 2017, **13**, 5481–5490.

58 A. J. Vromans and L. Giomi, *Soft matter*, 2016, **12**, 6490–6495.